Articles

Nitrogen-to-Metal Multiple Bond Functionalities: The Reaction of Calix[4]arene−W(IV) with Azides and Diazoalkanes

Geoffroy Guillemot, Euro Solari, and Carlo Floriani*

Institut de Chimie Minérale et Analytique, BCH, Université de Lausanne, CH-1015 Lausanne, Switzerland

Corrado Rizzoli

Dipartimento di Chimica, Università di Parma, I-43100 Parma, Italy

Received July 17, 2000

The [{calix[4]-$(O)_4$}W(η^2-C_6H_{10})], **2**, has been used as a source of W^{IV}-d^2 center-bonded to an oxo surface, which has been modeled by the calix[4]arene tetraanion in the reaction with diazoalkanes and organic azides. The olefin is easily displaced by both substrates. The reaction with Ph_2CN_2 led to the formation of metallahydrazone, [{calix[4]-$(O)_4$}W═N−$NCPh_2$], **5**, which binds Bu^tNC inside the cavity, **6**, or it can be reduced to a dinuclear W^V derivative [W−W, 2.646(1) Å], where the two metals are bridged by a diphenylhydrazido ligand in complex **7**, [{calix[4]-$(O)_4$}$_2W_2$(μ-N−N═CPh_2)$_2Na_2$]. The reaction of **2** with organic azides (RN_3) is strongly dependent on the nature of the R substituent at the azide functionality. The reaction with RN_3 [R = $SiMe_3$; CPh_3] occurs at the metal in the exo position, leading to alkylimido derivatives [{calix[4]-$(O)_4$}W═N−R] [R = $SiMe_3$, **8**; R = CPh_3, **9**], which bind inside the cavity Bu^tNC, leading to **10** and **11**, respectively. The reaction of **2** with PhN_3, on the contrary, occurs inside the calixarene cavity, leading to the triazenido derivative [{μ-calix[4]-$(O)_4$}$_2$(W═N−N═$NPh)_2$], **12**. The results of **2** with organic azides show that two different pathways are followed at the metal in the exo and endo positions. In the former case, for steric reasons, the 1,3 dipolar addition of the azide to the carbenoid metal precedes the formation of the alkylimido. In the case of PhN_3, the size of the calix cavity prevents the same pathway. In the case of HN_3 the reaction is supposed to proceed with HN_3 binding the metal with the protonated nitrogen inside the cavity and decomposing to the imido functionality [{μ-calix[4]-$(O)_4$}$_2$(W═$NH)_2$], **13**. An alternative synthetic route to arylimido derivatives of W^{VI} has been reported. The reaction of [calix[4]-$(ONa)_4(THF)_2$] with [*p*-tolyl-N≡WCl_4] led to [μ-calix[4]-W≡N-*p*-tolyl], **14**, which is in equilibrium in solution with the corresponding dimeric form [{μ-calix[4]}$_2$-W≡N-*p*-tolyl], **15**.

Introduction

A set of oxygen donor atoms, providing both σ and π electron donation to a metal center, is not appropriate for stabilizing any low oxidation state of a transition metal. This is, however, a synthetic advantage, since very reactive, unstable, low-valent metals produced in an oxygen donor atom environment can be generated in situ and intercepted by an appropriate reducible substrate. This event is probably occurring on metal-oxo surfaces displaying reactivities that are difficult to match using molecular compounds.[1] In this respect, metallacalixarenes are probably appropriate molecules for entering the game.[2] Reduction of metallacalixarenes,[3] namely in the case of tungsten[4] and niobium,[5]

* To whom correspondence should be addressed.

(1) (a) Thomas, J. M.; Thomas, W. J. *Principles and Practice of Heterogeneous Catalysis*; VCH: Weinheim, Germany, 1997. (b) Gates, B. *Catalytic Chemistry*; Wiley: New York, 1992. (c) *Mechanisms of Reactions of Organometallic Compounds with Surfaces;* Cole-Hamilton, D. J., Williams, J. O., Eds.; Plenum: New York, 1989. (d) Kung, H. H. *Transition Metal Oxides: Surface Chemistry and Catalysis*; Elsevier: Amsterdam, The Netherlands, 1989. (e) Hoffmann, R. *Solid and Surfaces, A Chemist's View of Bonding in Extended Strucures*; VCH: Weinheim, Germany, 1988. (f) Campbell, I. M. *Catalysis at Surfaces*; Chapman & Hall: London, U.K., 1988.

(2) Floriani, C. *Chem. Eur. J.* **1999**, *5*, 19.

(3) (a) Gutsche, C. D. *Calixarenes*; The Royal Society of Chemistry: Cambridge, U.K., 1989. (b) Gutsche, C. D. *Calixarene Revisited*; The Royal Society of Chemistry: Cambridge, U.K., 1998. (c) *Calixarenes, A Versatile Class of Macrocyclic Compounds*; Vicens, J., Böhmer, V., Eds.; Kluwer: Dordrecht, The Netherlands, 1991. (d) Bohmer, V. *Angew. Chem., Int. Ed. Engl.* **1995**, *34*, 713. (e) Wieser, C.; Dieleman, C. B.; Matt, D. *Coord. Chem. Rev.* **1997**, *165*, 93. (f) Roundhill, D. M. Metal Complexes of Calixarenes. In *Progr. Inorg. Chem.* **1995**, 533. (g) Ikeda, A.; Shinkai, S. *Chem. Rev.* **1887**, *97*, 1713.

(4) Giannini, L.; Solari, E.; Floriani, C.; Re, N.; Chiesi-Villa A.; Rizzoli, C. *Inorg. Chem.* **1999**, *38*, 1438.

10.1021/om000612s CCC: $20.00
Publication on Web 01/23/2001

led, in the absence of a suitable substrate, to the formation of metal−metal bonded dimers. Rarely does such a metal−metal functionality behave as a very reactive species.[5] One of the valid approaches to low-valent reactive fragments has been found reducing the metallacalixarene in the presence of an olefin,[6] which is, in many cases, a particularly labile ligand. This report concerns the use of a [W(IV)-calix[4]arene]−olefin complex as a source of the [d^2-W(IV)-calix[4]arene] fragment in the reaction with diazoalkanes and azides. Such reactions led either to the two-electron reduction of the substrate[7a] or to the cleavage of nitrogen−nitrogen multiple bonds with the formation of metal−imido species.[7] The reduction of diazoalkanes[8] and organic azides has been chosen for its relationship with the N_2 reduction and N−N bond cleavage, in general. The preorganized O_4 coordination environment, which makes available at the metal a σ and two π frontier orbitals, is a determining factor in such chemistry.[2]

Experimental Section

General Procedure. All reactions were carried out under an atmosphere of purified nitrogen. Solvents were dried and distilled before use by standard methods. ^{1}H NMR and IR spectra were recorded on AC-200, DPX-400 Bruker, and Perkin-Elmer FT 1600 instruments, respectively. The synthesis of [*cis*-Cl_2{*p*-Bu^t-calix[4]-$(O)_4$}W] was performed as reported.[4]

Synthesis of 1. Cyclopentene (4.63 g, 68.0 mmol) and Na (0.59 g, 25.7 mmol) were suspended in THF (200 mL) at −30 °C. [*cis*-Cl_2{*p*-Bu^t-calix[4]-$(O)_4$}W]·2(C_7H_8) (14.2 g, 13.1 mmol) was added, and the reaction mixture was stirred overnight while slowly warming to room temperature, giving a suspension of a white solid in a dark brown solution. The solid was filtered off, volatiles were removed in vacuo, toluene (50 mL) was added to the residue, and the volatiles evaporated again. The residue was dissolved in toluene (150 mL), and the solution was allowed to stand at room temperature for 6 h. Some solid was filtered off, and toluene was evaporated to dryness to give a brown microcrystalline solid, which was washed with *n*-pentane (50 mL) and dried in vacuo (5.16 g, 42.3%). Anal. Calcd for **1**·0.5(C_5H_{12}), $C_{51.5}H_{66}O_4W$: C, 66.30; H, 7.13. Found: C, 66.11; H, 7.07. ^{1}H NMR (C_6D_6, 400 MHz, 298 K, ppm): δ 7.06 (s, 8H, ArH); 5.34 (m, 2H, C_5H_8); 5.19 (m, 2H, C_5H_8); 4.60 (d, 4H, J = 12.2 Hz, *endo*-CH_2); 4.01 (m, 2H, C_5H_8); 3.15 (d, 4H, J = 12.2 Hz, *exo*-CH_2); 1.61 (m, 2H, C_5H_8); 1.10 (s, 36H, Bu^t overlapping with m, pentane); 0.86 (m, 3H, pentane).

Synthesis of 2. Cyclohexene (5.77 g, 70.2 mmol) and Na (0.84 g, 36.7 mmol) were suspended in THF (350 mL) at −50 °C and then degassed (vac/N_2 cycles). [*cis*-Cl_2{*p*-Bu^t-calix[4]-$(O)_4$}W]·2.3(C_7H_8) (20.5 g, 18.4 mmol) was added, and the reaction mixture was stirred overnight while slowly warming to room temperature, giving a suspension of a white solid in a brown-red solution. The solid was filtered off. The THF was evaporated to dryness to give a brown-orange residue, which was washed with Et_2O (100 mL) and dried in vacuo, giving **2**·($C_4H_{10}O$) (11.04 g, 61%). Anal. Calcd for **2**, $C_{54}H_{72}O_5W$: C, 65.85; H, 7.37. Found: C, 65.89; H, 7.37. ^{1}H NMR ($CDCl_3$, 400 MHz, 298 K, ppm): δ 7.11 (s, 8H, ArH); 4.64 (m, 2H, C_6H_{10}); 4.35 (d, 4H, J = 12.4 Hz, *endo*-CH_2); 4.26 (m, 2H, C_6H_{10}); 4.18 (m, 2H, C_6H_{10}); 3.46 (m, 4H, Et_2O); 3.23 (d, 4H, J = 12.4 Hz, *exo*-CH_2); 1.61 (m, 2H, C_6H_{10}); 1.44 (m, 2H, C_6H_{10}); 1.21 (s, 36H, Bu^t) overlapping with 1.19 (m, 6H, Et_2O). ^{13}C NMR ($CDCl_3$, 100.6 MHz, 298 K, ppm): δ 156.0 (Ar *C*O); 146.4 (Ar *C*Bu^t); 131.8 (Ar *C*); 125.0 (Ar *C*H); 82.2 (*C*H); 34.2 (*C*$(CH_3)_3$); 33.7 (*C*H_2 of calix); 31.4 (C(*C*$H_3)_3$); 26.6 (*C*H_2 of cyclohexene); 22.4 (*C*H_2 of cyclohexene).

Synthesis of 3. *tert*-Butylisocyanide (0.6 g, 7.24 mmol) was added to a suspension of **1**·0.5(C_5H_{12}) (5.47 g, 5.86 mmol) in toluene (80 mL) at room temperature. The mixture was stirred for 5 h and then allowed to stand overnight at room temperature. The resulting brown solid was collected and dried in vacuo (3.25 g, 49.6%). Anal. Calcd for **3**·1.5(C_7H_8), $C_{64.5}H_{81}NO_4W$: C, 69.28; H, 7.30; N, 1.2. Found: C, 69.29; H, 7.40; N, 1.23. ^{1}H NMR (C_6D_6, 200 MHz, 298 K, ppm): δ 7.15−6.98 (m, 7.5H, tol) overlapping with 7.09 (s, 8H, ArH); 6.06 (m, 2H, C_5H_8); 5.98 (m, 2H, C_5H_8); 4.79 (d, 4H, J = 12.4 Hz, *endo*-CH_2); 4.33 (m, 2H, C_5H_8); 3.19 (d, 4H, J = 12.4 Hz, *exo*-CH_2); 2.10 (s, 4.5H, toluene); 1.90−1.67 (m, 2H, C_5H_8); 1.24 (s, 36H, Bu^t); −0.20 (s, 9H, Bu^{t}NC).

Synthesis of 4. A solution of *tert*-butylisocyanide (0.29 g, 3.49 mmol) in toluene (30 mL) was added dropwise to a suspension of **2**·($C_4H_{10}O$) (3.52 g, 3.57 mmol) in toluene (90 mL) at −20 °C. The mixture was stirred overnight, while slowly warming to room temperature. The resulting brown suspension was concentrated in vacuo to ca. 20 mL, and *n*-hexane (40 mL) was added, giving light brown **4**·2(C_7H_8), which was collected and dried in vacuo (3.46 g, 82%). Anal. Calcd for **4**·2(C_7H_8), $C_{69}H_{87}NO_4W$: C, 70.34; H, 7.44; N, 1.19. Found: C, 70.23; H, 7.46; N, 0.99. ^{1}H NMR (C_6D_6, 400 MHz, 298 K, ppm): δ 7.15−6.99 (m, 10H, tol) overlapping with 7.09 (s, 8H, ArH); 5.45 (m, 2H, C_6H_{10}); 5.30 (m, 2H, C_6H_{10}); 5.02 (m, 2H, C_6H_{10}); 4.80 (d, 4H, J = 12.3 Hz, *endo*-CH_2); 3.19 (d, 4H, J = 12.3 Hz, *exo*-CH_2); 2.10 (s, 6H, tol); 1.70 (m, 4H, C_6H_{10}); 1.24 (s, 36H, Bu^t); −0.19 (s, 9H, Bu^{t}NC). IR (Nujol, ν_{max}/cm^{-1}): 2211.8 (s). IR (Nujol, ν_{max}/cm^{-1}): 2211.8 (s), 1756 (w), 1594 (w), 1461 (s br), 1362 (m); 1294 (s), 1242 (m), 1193 (s), 1152 (m); 1104 (m); 919 (m), 874 (s), 851 (s), 824 (s), 798 (s), 753 (m), 727 (m); 630 (W); 568 (m), 542 (m).

Synthesis of 5. A suspension of **2**·($C_4H_{10}O$) (3.14 g, 3.19 mmol) in THF (90 mL) was added to a solution of diphenyldiazomethane (0.69 g, 3.55 mmol) in Et_2O (40 mL) at −60 °C. The reaction mixture was stirred overnight while slowly warming to room temperature. The resulting red-orange suspension was stirred at room temperature for 1 day, before collecting and drying in vacuo **5**·(C_4H_8O) (1.83 g, 52.5%). Anal. Calcd for **5**·(C_4H_8O), $C_{61}H_{70}N_2O_5W$: C, 66.91; H, 6.44; N, 2.56. Found: C, 66.56; H, 6.55; N, 2.39. ^{1}H NMR (Tol-d_8, 400 MHz, 298 K, ppm): δ 7.65 (m, 4H, $(C_6H_5)_2CN_2$); 7.20 (m, 2H, $(C_6H_5)_2CN_2$); 7.12 (s, ArH overlapping with signal due to deuterated solvent); 7.04 (m, 4H, $(C_6H_5)_2CN_2$); 4.64 (d, 4H, J = 12.3 Hz, *endo*-CH_2); 3.55 (m, 4H, THF); 3.20 (d, 4H, J = 12.3 Hz, *exo*-CH_2); 1.45 (m, 4H, THF); 1.12 (s, 36H, Bu^t). IR (Nujol, ν_{max}/cm^{-1}): 1756 (w), 1594 (w), 1511 (m); 1456 (s br), 1378 (s); 1361 (m); 1328 (m); 1300 (m), 1250 (m), 1200 (s br), 1122 (m); 917 (m), 872 (w), 833 (m), 800 (m), 750 (m), 722 (m); 694 (m), 556 (m).

Synthesis of 6. Complex **5** reacts with *tert*-butylisocyanide in a 1:1 ratio to give **6**, as determined by NMR. ^{1}H NMR (Tol-d_8, 400 MHz, 298 K, ppm): δ 7.82 (m, 2H, $(C_6H_5)_2CN_2$); 7.62 (m, 2H, $(C_6H_5)_2CN_2$); 7.20 (m, 2H, $(C_6H_5)_2CN_2$); 7.11 (s, 8H, ArH); 7.02 (m, 4H, $(C_6H_5)_2CN_2$); 4.96 (d, 4H, J = 12.5 Hz, *endo*-CH_2); 3.28 (d, 4H, J = 12.5 Hz, *exo*-CH_2); 1.22 (s, 36H, Bu^t); −0.26 (s, 9H, Bu^{t}NC). IR (Nujol, ν_{max}/cm^{-1}): 2211.5 (s). Anal. Calcd for **6**, $C_{62}H_{71}N_3O_4W$: C, 67.32; H, 6.47; N, 3.80. Found: C, 67.47; H, 6.57; N, 3.91.

Synthesis of 7. Na (86 mg, 3.74 mmol) and **5**·0.5($C_4H_{10}O$) (3.98 g, 3.75 mmol) were suspended in THF (220 mL), and the reaction mixture was stirred overnight. The resulting orange suspension was evaporated to dryness to give a light orange

(5) Caselli, A.; Solari, E.; Scopelliti, R.; Floriani, C.; Re, N.; Rizzoli, C.; Chiesi-Villa, A. *J. Am. Chem. Soc.* **2000**, *122*, 3652.
(6) Giannini, L.; Guillemot, G.; Solari, E.; Floriani, C.; Chiesi-Villa, A.; Rizzoli, C. *J. Am. Chem. Soc.* **1999**, *121*, 2797.
(7) (a) Wigley, D. E. *Progr. Inorg. Chem.* **1994**, *42*, 239. (b) Nugent, W. A.; Mayer, J. M. *Metal−Ligand Multiple Bonds;* Wiley-Interscience: New York, 1988.
(8) Sutton, D. *Chem. Rev.* **1993**, *93*, 995.

residue, which was washed with Et_2O (70 mL) and dried in vacuo to give **7**·4($C_4H_{10}O$) (2.65 g, 59%). Anal. Calcd for **7**·4($C_4H_{10}O$), $C_{130}H_{164}N_4Na_2O_{12}W_2$: C, 65.37; H, 6.92; N, 2.35. Found: C, 65.32; H, 6.66; N, 2.40. ^{1}H NMR (Pyr-d_5, 400 MHz, 298 K, ppm): δ 7.51 (m, 4H, $(C_6H_5)_2CN_2$); 7.41−7.24 (m, 16H, $(C_6H_5)_2CN_2$) overlapping with 7.24 (m, 4H, ArH); 7.02 (m, 8H, ArH); 6.67 (m, 4H, ArH); 5.12 (d, 4H, J = 12.9 Hz, *endo*-CH_2); 3.85 (d, 4H, J = 13.5 Hz, *endo*-CH_2); 3.38 (d, 4H, *exo*-CH_2) overlapping with 3.33 (m, 16H, Et_2O); 2.69 (d, 4H, J = 13.5 Hz, *exo*-CH_2); 1.13 (s, 36H, Bu^t) overlapping with (m, 24H, Et_2O); 0.97 (s, 18H, Bu^t); 0.84 (s, 18H, Bu^t). IR (Nujol, ν_{max}/cm^{-1}): 1739 (w), 1594 (w); 1511 (w); 1456 (s br), 1378 (m); 1361 (m); 1317 (s); 1300 (s); 1283 (s), 1250 (m), 1205 (s br), 1122 (m); 917 (m), 839 (m), 767 (s), 694 (m), 644 (m), 556 (m); 417 (m). Crystals suitable for an X-ray analysis were obtained in a THF/Et_2O solution at −20 °C.

Synthesis of 8. Compound **2**·($C_4H_{10}O$) (2.1 g, 2.13 mmol) was added to a solution of Me_3SiN_3 (0.24 g, 2.08 mmol) in benzene (100 mL) at room temperature. The brown reaction mixture was stirred for 1 h and then heated at 60 °C for 3 h. Volatiles were evaporated to dryness to give a yellow solid that was washed with *n*-pentane (40 mL) to yield 1.46 g (69.3%) of **8**·(C_5H_{12}). Anal. Calcd for **8**·(C_5H_{12}), $C_{52}H_{73}NO_4SiW$: C, 63.21; H, 7.45; N, 1.42. Found: C, 63.07; H, 7.58; N, 1.15. ^{1}H NMR ($CDCl_3$, 200 MHz, 298 K, ppm): δ 7.10 (s, 8H, ArH); 4.57 (d, 4H, J = 12.3 Hz, *endo*-CH_2); 3.26 (d, 4H, J = 12.3 Hz, *exo*-CH_2); 1.25 (m, 6H, pentane) overlapping with 1.21 (s, 36H, Bu^t); 0.88 (m, 6H, pentane); 0.50 (s, 9H, $(CH_3)_3$Si). ^{13}C NMR ($CDCl_3$, 100.6 MHz, 298 K, ppm): δ 151.59 (Ar *C*O); 145.89 (Ar *C*^{t}Bu); 130.84 (Ar *C*); 124.94 (Ar *C*H); 34.14 (*C*$(CH_3)_3$); 33.62 (*C*H_2); 31.48 (C(*C*$H_3)_3$); 0.63 (NSi(*C*$H_3)_3$). IR (Nujol, ν_{max}/cm^{-1}): 1750 (w), 1578 (w), 1462 (s br), 1306 (m), 1286 (m), 1250 (s), 1167 (s br), 1106 (s), 917 (m), 872 (m), 828 (s br), 798 (m), 762 (m); 678 (m), 631 (w); 556 (s); 503 (w); 422 (s). Crystals suitable for an X-ray analysis were grown from a toluene solution.

Synthesis of 9. Ph_3CN_3 (0.93 g, 3.26 mmol) and **2**·($C_4H_{10}O$) (2.9 g, 2.94 mmol) were suspended in toluene (110 mL), and the resulting mixture was heated at 60 °C overnight, giving a dark red-violet suspension. Volatiles were evaporated to dryness. The violet residue was washed with Et_2O (30 mL) and dried in vacuo to give **9**·($C_4H_{10}O$)·0.5(C_7H_8) (0.46 g, 13%). The compound was isolated in a low yield due to its high solubility in organic solvents. Anal. Calcd for **9**·($C_4H_{10}O$)·0.5(C_7H_8), $C_{70.5}H_{81}NO_5W$: C, 70.20; H, 6.77; N, 1.16. Found: C, 70.42; H, 6.99; N, 1.54. ^{1}H NMR ($CDCl_3$, 400 MHz, 298 K, ppm): δ 7.62 (m, 6H, $(C_6H_5)_3$CN); 7.38 (m, 6H, $(C_6H_5)_3$CN); 7.36−7.16 (m, $(C_6H_5)_3$CN overlapping with signals due to deuterated solvent and toluene); 7.09 (s, 8H, ArH); 4.48 (d, 4H, J = 12.2 Hz, *endo*-CH_2); 3.47 (m, 4H, Et_2O); 3.23 (d, 4H, J = 12.2 Hz, *exo*-CH_2); 2.35 (s, 1.5H, tol); 1.20 (s, 36H, Bu^t overlapping with m, 6H, Et_2O). ^{13}C NMR ($CDCl_3$, 100.6 MHz, 298 K, ppm): δ 152 (Ar *C*O); 145.81 (Ar *C*Bu^t); 130.78 (Ar *C*); 128.91 (Ar *C*H of NC($C_6H_5)_3$); 128.18 (Ar *C*H of NC($C_6H_5)_3$); 127.62 (Ar *C*H of NC($C_6H_5)_3$); 124.93 (Ar *C*H); 34.05 (*C*$(CH_3)_3$); 33.68 (*C*H_2); 31.49 (C(*C*$H_3)_3$). IR (Nujol, ν_{max}/cm^{-1}): 1811 (w); 1778 (W); 1756 (w), 1600 (w), 1467 (s br), 1361 (m), 1305 (m), 1283 (m), 1261 (s br); 1194 (s br), 1105 (m), 1033 (w); 922 (m), 839 (s), 800 (s), 761 (m), 700 (m); 639 (w), 561 (m); 422 (m).

Synthesis of 10. *tert*-Butylisocyanide (0.11 g, 1.32 mmol) was added to a solution of **8**·(C_5H_{12}) (1.33 g, 1.35 mmol) in toluene (100 mL) and stirred for 1 day at room temperature. Volatiles of the resulting mixture were evaporated, and the light brown residue was washed with *n*-pentane (30 mL) and dried in vacuo to give **10**·(C_5H_{12}) (1.12 g, 77.7%). Anal. Calcd for **10**·(C_5H_{12}), $C_{57}H_{82}N_2O_4SiW$: C, 63.91; H, 7.72; N, 2.62. Found: C, 63.74; H, 7.63; N, 2.87. ^{1}H NMR ($CDCl_3$, 400 MHz, 298 K, ppm): δ 7.06 (s, 8H, ArH); 4.73 (d, 4H, J = 12.5 Hz, *endo*-CH_2); 3.28 (d, 4H, J = 12.5 Hz, *exo*-CH_2); 1.24 (m, 6H, pentane); 1.19 (s, 36H, Bu^t); 0.87 (m, 6H, pentane); 0.43 (s, 9H, $(CH_3)_3$Si); −0.24 (s, 9H, Bu^{t}NC). ^{13}C NMR ($CDCl_3$, 100.6 MHz, 298 K, ppm): δ 158.86 (Ar *C*O); 144.07 (Ar *C*Bu^t); 129.18 (Ar *C*); 124.95 (Ar *C*H); 53.97 ((CH$_3)_3$CNC); 33.96 (*C*$(CH_3)_3$); 33.71 (*C*H_2); 31.72 (C(*C*$H_3)_3$); 29.46 ((*C*H$_3)_3$CNC); 0.62 (NSi(*C*$H_3)_3$). IR (Nujol, ν_{max}/cm^{-1}): 2211.1 (s); 1756 (w), 1572 (w), 1456 (s br), 1378 (m); 1361 (m); 1306 (s), 1289 (s), 1244 (s), 1194 (s); 1150 (s br), 1122 (s); 1106 (s), 916 (m), 874 (m), 848 (s br), 798 (s), 760 (m); 730 (m); 678 (m), 633 (m); 556 (s); 502 (m); 422 (s).

Synthesis of 11. *tert*-Butylisocyanide was reacted with **10**·($C_4H_{10}O$)·0.5(C_7H_8) in a 1:1 ratio to give the derived compound **11**, as determined by NMR. ^{1}H NMR ($CDCl_3$, 200 MHz, 298 K, ppm): δ 7.65 (m, 6H, $(C_6H_5)_3$CN); 7.34 (m, 6H, $(C_6H_5)_3$CN); 7.33−7.17 (m, $(C_6H_5)_3$CN overlapping with solvents); 7.07 (s, 8H, ArH); 4.67 (d, 4H, J = 12.4 Hz, *endo*-CH_2); 3.26 (d, 4H, J = 12.4 Hz, *exo*-CH_2); 1.19 (s, 36H, Bu^t); −0.24 (s, 9H, Bu^{t}NC).

Synthesis of 12. A solution of PhN_3 (0.25 g, 2 mmol) in toluene (40 mL) was added dropwise to a solution of **2**·($C_4H_{10}O$) (2 g, 2.03 mmol) in toluene (90 mL), and the solution was stirred overnight at room temperature. The resulting red microcrystalline suspension was heated at 110 °C for 3 h. Volatiles were evaporated to dryness to give a red microcrystalline solid, which was washed with *n*-pentane (40 mL) and dried in vacuo to give **12** (1.59 g, 82.5%). Anal. Calcd for **12**, $C_{100}H_{114}N_6O_8W_2$: C, 63.36; H, 6.06; N, 4.43. Found: C, 63.27; H, 6.12; N, 4.32. ^{1}H NMR ($CDCl_3$, 200 MHz, 298 K, ppm): δ 7.24 (s, due to deuterated solvent) overlapping with 7.23 (s, 4H, ArH); 7.13 (s, 4H, ArH); 7.05−6.95 (m, 6H, $C_6H_5N_3$ overlapping with m, 4H, ArH); 6.92 (m, 4H, ArH); 6.28 (m, 4H, $C_6H_5N_3$); 6.10 (d, 4H, J = 13.2 Hz, *endo*-CH_2); 4.75 (d, 4H, J = 13.2 Hz, *endo*-CH_2); 3.56 (d, 4H, J = 13.2 Hz, *exo*-CH_2); 3.41 (d, 4H, J = 13.2 Hz, *exo*-CH_2); 1.25 (s, 18H, Bu^t); 1.21 (s, 18H, Bu^t); 0.84 (s, 36H, Bu^t). ^{13}C NMR ($CDCl_3$, 100.6 MHz, 298 K, ppm): δ 170.61 (Ar *C*O); 168.07 (Ar *C*O); 160.19 (Ar *C*O); 147.21 (Ar C_q of $C_6H_5N_3$); 146.46 (Ar *C*Bu^t); 145.40 (Ar *C*Bu^t); 144.41 (Ar *C*Bu^t); 133.01 (Ar C_q); 132.24 (Ar *C*H of $C_6H_5N_3$); 129.32 (Ar C_q); 127.64 (Ar *C*H of $C_6H_5N_3$); 127.18 (Ar C_q); 126.22 (Ar *C*H); 124.81 (Ar *C*H); 124.09 (Ar *C*H); 123.91 (Ar *C*H); 123.07 (Ar *C*H of $C_6H_5N_3$); 34.07 (*C*$(CH_3)_3$); 33.90 (*C*$(CH_3)_3$); 33.53 (*C*H_2); 32.96 (*C*H_2); 31.78 (C(*C*$H_3)_3$); 31.54 (C(*C*$H_3)_3$); 31.25 (C(*C*$H_3)_3$). IR (Nujol, ν_{max}/cm^{-1}): 1739 (w), 1594 (w), 1456 (s br), 1394 (m); 1361 (m); 1289 (s), 1256 (m), 1183 (s br), 1117 (m); 1100 (m); 1022 (w); 911 (m), 867 (m), 822 (s), 794 (s), 744 (m), 689 (m), 617 (m), 572 (m); 556 (s); 517 (s); 482 (m). Crystals suitable for an X-ray analysis were grown in a toluene/heptane solution. *tert*-Butylisocyanide does not react with **12**.

Synthesis of 13. Method A. Compound **2**·($C_4H_{10}O$) (7.75 g, 7.87 mmol) and $(Ph)(Me)_2CN_3$ (1.27 g, 7.88 mmol) were suspended in benzene (240 mL), and the mixture was stirred at 60 °C overnight. The obtained yellow solid was collected, washed with *n*-hexane (40 mL), and dried in vacuo to yield 4.92 g (67.8%) of **13**·2(C_6H_6). α-Methylstyrene was detected by gas chromatography and characterized by mass spectroscopy in mother liquor volatiles. Anal. Calcd for **13**·2(C_6H_6), $C_{100}H_{118}N_2O_8W_2$: C, 65.14; H, 6.45; N, 1.52. Found: C, 65.11; H, 6.41; N, 1.50. Crystals suitable for an X-ray analysis were grown in a chlorobenzene solution at −20 °C.

Method B. HN_3 (12.5 mL, 0.222 N in Et_2O, 2.77 mmol) was added dropwise to a toluene (110 mL) suspension of **2**·($C_4H_{10}O$) (2.45 g, 2.49 mmol) at −70 °C. The reaction mixture was stirred overnight while slowly warming to room temperature, giving a suspension of a yellow solid in a red solution. The solid was collected, washed with *n*-hexane (40 mL), and dried in vacuo to yield 1.77 g (76%) of **13**·2(C_7H_8). Anal. Calcd for **13**·2(C_7H_8), $C_{102}H_{122}N_2O_8W_2$: C, 65.45; H, 6.57; N, 1.50. Found: C, 65.85; H, 6.59; N, 1.45. ^{1}H NMR ($CDCl_3$, 400 MHz, 298 K, ppm): δ 7.26−7.12 (m, toluene) overlapping with 7.19 (m, 4H, ArH) and 7.16 (m, 4H, ArH); 7.11 (m, 8H, ArH); 6.16 (d, 4H, J = 12.8 Hz, *endo*-CH_2); 4.74 (d, 4H, J = 12.8 Hz, *endo*-CH_2); 3.51 (d, 4H, J = 12.8 Hz, *exo*-CH_2); 3.40 (d, 4H, J = 12.8 Hz, *exo*-CH_2); 2.88 (br d, 2H, *endo*-HN); 2.34 (s, 6H, toluene);

Table 1. Experimental Data for the X-ray Diffraction Studies on Crystalline Complexes 7, 8, 12, 13, and 15

	7	8	12	13	15
formula	$C_{130}H_{156}N_4Na_2O_{12}W_2\cdot 6C_4H_8O$	$C_{47}H_{61}NO_4SiW\cdot 2C_7H_8$	$C_{100}H_{114}N_6O_8W_2\cdot 3C_7H_8$	$C_{88}H_{106}N_2O_8W_2\cdot 8C_6H_5Cl$	$C_{102}H_{118}N_2O_8W_2\cdot 3CHCl_3$
a, Å	17.074(2)	14.761(2)	17.262(4)	13.601(1)	13.030(4)
b, Å	19.511(3)	20.563(2)	17.954(4)	15.674(2)	18.267(2)
c, Å	24.687(3)	19.726(2)	21.931(4)	17.173(2)	21.776(4)
α, deg	107.90(2)	90	80.13(2)	66.14(2)	90
β, deg	98.60(2)	90	79.70(2)	67.61(2)	97.44(2)
γ, deg	104.63(2)	90	61.56(2)	73.04(2)	90
V, Å^3	7338(2)	5987.4(12)	5851(2)	3054.4(8)	5139.5(19)
Z	2	4	2	1	2
fw	2813.0	1100.2	2172.2	2588.0	2225.9
space group	$P\bar{1}$ (no. 2)	$Cmc2_1$ (no. 36)	$P\bar{1}$ (no. 2)	$P\bar{1}$ (no. 2)	$P21/c$ (no. 14)
T, °C	−130	−130	293	−130	293
λ, Å	0.71069	0.71069	0.71069	0.71069	0.71069
ρ_{calc}, g cm^{-3}	1.273	1.221	1.233	1.407	1.438
μ, cm^{-1}	16.65	20.30	20.58	21.54	25.73
transmn coeff	0.897−1.000	0.977−1.000	0.857−1.000	0.837−1.000	0.836−1.000
$R^{a,b}$	0.095	0.035 [0.054]	0.098	0.043	0.073
$wR_2{}^c$	0.220	0.079 [0.130]	0.240	0.106	0.188
GOF	1.308	1.097	1.089	1.074	1.055
N-observed[d]	17 353	6649	9888	7487	7435
N-independent[e]	29 139	7717	19 816	8036	10 909
N-refinement[f]	17 353	6649	9888	7487	7435
no. of variables	1537	332	1166	583	568

[a] Calculated on the unique observed data having $I > 2\sigma(I)$ for **13**; $I > 3\sigma(I)$ for **8**, **12**, **15**; $I > 4\sigma(I)$ for **7**. [b] Values in square brackets refer to the "inverted" structure. [c] Calculated on the unique data with $I > 2\sigma(I)$ for **13**; with $I > 3\sigma(I)$ for **8**, **12**, **15**; $I > 4\sigma(I)$ for **7**. [d] *N*-observed is the total number of independent reflections having $I > 2\sigma(I)$ for **13**; $I > 3\sigma(I)$ for **8**, **12**, **15**, $I > 4\sigma(I)$ for **7**. [e] *N*-independent is the number of independent reflections. [f] *N*-refinement is the number of reflections used in the refinement having $I > 2\sigma(I)$ for **13**; $I > 3\sigma(I)$ for **8**, **12**, **15**; $I > 4\sigma(I)$ for **7**.

1.21 (s, 36H, Bu^t overlapping with s, 18H, Bu^t); 1.20 (s, 18H, Bu^t). ^{13}C NMR ($CDCl_3$, 100.6 MHz, 298 K, ppm): δ 172.72 (Ar *C*O); 171.05 (Ar *C*O); 164.13 (Ar *C*O); 146.49 (Ar *C*Bu^t); 145.37 (Ar *C*Bu^t); 144.37 (Ar *C*Bu^t); 132.36 (Ar *C*); 129.83 (Ar *C*); 128.44 (Ar *C*); 127.34 (Ar *C*); 126.09 (Ar *C*H); 124.83 (Ar *C*H); 124.60 (Ar *C*H); 124.37 (Ar *C*H); 34.11 ($C(CH_3)_3$); 33.99 ($C(CH_3)_3$); 33.73 (CH_2); 33.27 (CH_2); 31.72 ($C(CH_3)_3$); 31.66 ($C(CH_3)_3$); 31.50 ($C(CH_3)_3$). IR (Nujol, ν_{max}/cm^{-1}): 3400 (s); 1750 (w), 1578 (w), 1461 (s br), 1378 (m); 1361 (m); 1289 (s), 1239 (m), 1183 (s br), 1117 (m); 1100 (m); 967 (m); 911 (m), 872 (m), 828 (s), 794 (s), 750 (m), 694 (m), 678 (s); 633 (m), 567 (m); 517 (s); 433 (m). *tert*-Butylisocyanide does not react with **13**.

Synthesis of 14 and 15. *p*-tolylNWCl$_4$ (3.84 g, 8.91 mmol) and [*p*-Bu^t-calix[4]-(O)$_4$(Na)$_4$]·2(C_4H_8O) (8.27 g, 9.39 mmol) were suspended in THF (350 mL), and the mixture was stirred overnight at 60 °C, giving a suspension of a white solid in a red solution. The solid was filtered off, and volatiles were evaporated to dryness. The orange residue was washed with Et_2O (60 mL) and dried in vacuo to yield 6.4 g (68.8%) of **15**·2($C_4H_{10}O$)·(C_4H_8O). ^{1}H NMR spectra showed a mixture of monomeric high symmetric and dimeric low symmetric forms: ^{1}H NMR (monomeric form **14**) ($CDCl_3$, 400 MHz, 298 K, ppm): δ 7.26 (m, 3H, $NC_6H_4CH_3$); 7.14 (m, 1H, $NC_6H_4CH_3$); 7.12 (s, 8H, ArH); 4.58 (d, 4H, J = 12.5 Hz, *endo*-CH_2); 3.28 (d, 4H, J = 12.5 Hz; *exo*-CH_2); 2.53 (s, 3H, $NC_6H_4CH_3$); 1.21 (s, 36H, Bu^t). ^{1}H NMR (dimeric form **15**) ($CDCl_3$, 400 MHz, 298 K, ppm): δ 7.16 (m, 4H, ArH); 7.04 (m, 4H, ArH); 6.76 (m, 4H, $NC_6H_4CH_3$); 6.72 (s, 8H, ArH); 6.36 (m, 4H, NC_6H_4-CH_3); 5.61 (d, 4H, J = 12.3 Hz, *endo*-CH_2); 4.73 (d, 4H, J = 14 Hz, *endo*-CH_2); 3.40 (d, 4H, J = 12.3 Hz, *exo*-CH_2); 3.34 (d, 4H, J = 14 Hz, *exo*-CH_2); 2.36 (s, 6H, $NC_6H_4CH_3$); 1.21 (s, 36H, Bu^t); 1.08 (s, 18H, Bu^t); 0.89 (s, 18H, Bu^t). Anal. Calcd for **15**·2($C_4H_{10}O$)·(C_4H_8O), $C_{114}H_{146}N_2O_{11}W_2$: C, 65.57; H, 7.05; N, 1.34. Found: C, 65.88; H, 6.69; N, 1.53. IR (Nujol, ν_{max}/cm^{-1}): 1750 (w), 1594 (w), 1494 (m); 1467 (s br), 1361 (m); 1300 (m), 1244 (m), 1194 (s br), 1125 (m), 1106 (m), 1020 (w); 982 (w); 917 (m), 872 (m), 833 (s), 800 (m), 750 (m); 679 (m), 550 (s); 531 (w); 433 (s). Crystals suitable for an X-ray analysis were grown from a $CHCl_3$ solution at room temperature.

Synthesis of 16. *tert*-Butylisocyanide reacts with **15** to give the derived compound **16**, as determined by NMR. ^{1}H NMR ($CDCl_3$, 400 MHz, 298 K, ppm): δ 7.31 (m, 2H, $NC_6H_4CH_3$); 7.27 (m, 2H, $NC_6H_4CH_3$); 7.08 (s, 8H, ArH); 4.79 (d, 4H, J = 12.5 Hz, *endo*-CH_2); 3.30 (d, 4H, J = 12.5 Hz; *exo*-CH_2); 2.55 (s, 3H, $NC_6H_4CH_3$); 1.20 (s, 36H, Bu^t); −0.23 (s, 9H, Bu^{t}NC). ^{13}C NMR ($CDCl_3$, 100.6 MHz, 298 K, ppm): δ 159.69 (Ar *C*O); 151.45 (Ar *C*N of N*p*-tolyl); 144.01 (Ar *C*^{t}Bu); 137.49 (Ar *C*CH_3 of N*p*-tolyl); 129.20 (Ar *C*); 128.24 (Ar *C*H of N*p*-tolyl); 128.00 (Ar *C*H of N*p*-tolyl); 125.15 (Ar *C*H)); 54.98 ((CH_3)$_3$CNC); 33.97 ($C(CH_3)_3$); 33.72 (CH_2); 31.89 ($C(CH_3)_3$); 29.23 ((CH_3)$_3$CNC); 21.09 (CH_3 of N*p*-tolyl). IR (Nujol, ν_{max}/cm^{-1}): 2211.1 (s) 1756 (w), 1600 (w), 1500 (m); 1461 (s br); 1361 (m); 1306 (m), 1289 (m), 1244 (m); 1194 (s br), 1106 (m), 1020 (w); 972 (w); 917 (m), 872 (m), 833 (s), 800 (s), 761 (m); 683 (w), 556 (s); 417 (s).

X-ray Crystallography. Single crystals suitable for X-ray diffraction were grown from common organic solvents (Table 1). Data for **12** and **15** were collected at 293 K on a Mar345 image plate. Those for **7** and **8** were collected at 143 K on a Kuma CCD, while those for **13** were collected at 143 K on a Rigaku AFC7S CCD using Mo Kα radiation. The solutions and refinements were carried out using the programs SHELX76[9] and SHELX93.[10] The details of the X-ray data collection, structure solutions, and refinements are given in the Supporting Information.[11]

Results and Discussion

The cyclopentene and cyclohexene derivatives of W^{IV}-calix[4]arene, [W-*p*-Bu^t-calix[4]-(O$_4$)], **1**, and **2** (Scheme 1)[6] are particularly appropriate sources of the d^2-W^{IV} fragment, due to the intrinsic lability of the olefin ligand. They have been prepared, as reported, reducing the [*cis*-Cl_2W{*p*-Bu^t-calix[4]-(O$_4$)}] in the presence of the appropriate olefins. In their absence, the d^2 fragment collapses, forming W═W dimers.[4] The lability of the

(9) Sheldrick, G. M. *SHELX76, Program for crystal structure determination*; University of Cambridge: England, 1976.
(10) Sheldrick, G. M. *SHELXL93, Program for crystal structure refinement*; University of Göttingen: Germany, 1993.
(11) See paragraph at the end of paper regarding Supporting Information.

Scheme 1

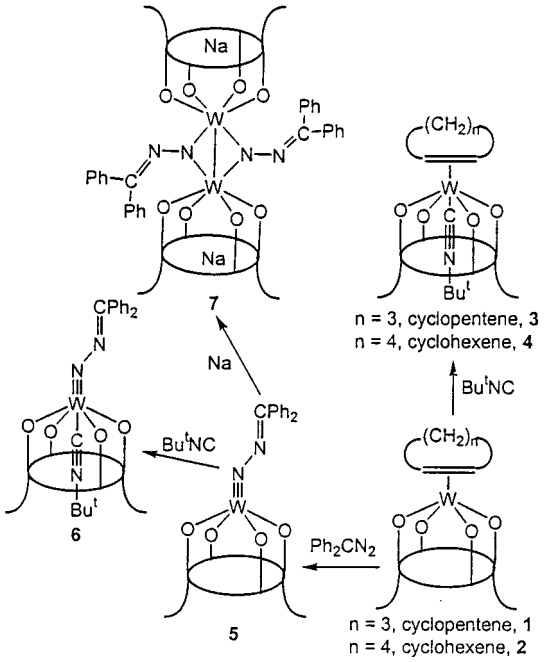

olefin ligand is considerably decreased in the corresponding isocyanide derivatives **3** and **4**, obtained in the reaction of **1** and **2** with Bu^{t}NC, which strongly stabilizes the W(olefin) functionality. The reaction of **1** or **2** with Ph_2CN_2 in THF led to the formation of **5**, where the diphenyldiazomethane has been reduced by two electrons,[8] as expected, in a reaction with a d^2 metal, thus forming a metallahydrazone. In **5**, the diazo group is bonded outside the calixarene cavity, and the exo conformation is chemically supported by the complexation of Bu^{t}NC to a very acidic center inside the cavity [ν_{CN}, 2211 cm^{-1}].

In the attempt to cleave reductively the N−N single bond, complex **5** was reduced with sodium metal.[5,8] The reaction proceeded, instead, with a reduction of the metal and a rearranged bonding mode of the hydrazonido functionality, as shown for complex **7** in Scheme 1. The formation of the W−W single bond [2.646(1) Å] forced the hydrazonido dianion to display a bridging bonding mode.[12] The ^{1}H NMR spectrum displays, differently from the solid-state structure in Figure 1, C_s symmetry (see the Experimental Section).

The six-coordination of the metal and the inclusion of the sodium cation completely remove the planarity of the O_4 core and the cone conformation of the calixarene, the opposite **A** and **C** rings being nearly parallel to each other and to the reference plane (Table 3). The W−W line forms dihedral angles of 166.8(2)° and 167.3(2)° with the normal to the mean "reference planes" of the calixarene units A and B, respectively. Coordination around the sodium cations is completed by two oxygen atoms from the THF molecule. In addition, the narrow range of the contact distances suggests the presence of η^6-interactions occurring between the alkali

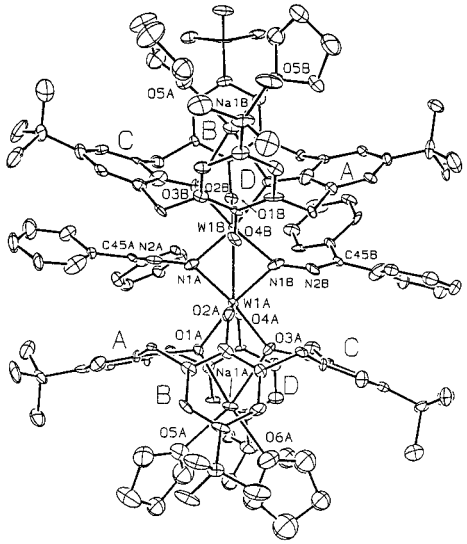

Figure 1. ORTEP drawing of complex **7** (50% probability ellipsoids). Disorder has been omitted for clarity.

Scheme 2

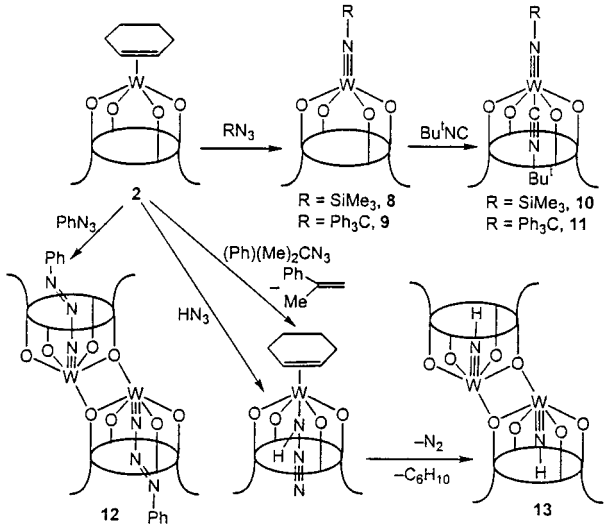

cations and the **B** and **D** aromatic rings.[13,14] The W−O(1) and W−O(3) bonds involving oxygen atoms bonded to sodium ions are longer [mean value 2.034(8) Å] than the W−O(2) and W−O(4) bond distances [mean value 1.967(11) Å]. The structural parameters related to the hydrazonido ligand support the proposed bonding scheme (Table 2).

In the case of organic azides, both the cleavage of N−N bonds and the two-electron reduction of the RN_3 functional group have been observed.[7,8] Which reaction takes place depends on the steric properties of the azide employed (see Scheme 2). The reaction of **2** with Me_3SiN_3 and Ph_3CN_3 follows, very probably, the same pathways leading to the formation of exo-alkylimido derivatives **8** and **9**, respectively, with the loss of dinitrogen. Both have been converted to the corresponding isocyanide derivatives **10** and **11**, upon reaction with Bu^{t}NC. The latter reaction has been used to support the

(12) (a) Curtis, M. D.; Messerle, L.; D'Errico, J. J.; Butler W. M.; Hay, M. S. *Organometallics* **1986**, *5*, 2283. (b) Messerle L.; Curtis, M. D. *J. Am. Chem. Soc.* **1980**, *102*, 7789.

(13) Na(1)A···C(8)A,C(13)A: 3.16(2)−3.81(2) Å; Na(1)A···C(22)A,C(27)A: 3.19(2)−3.97(2) Å; Na(1)B···C(8)B,C(13)B: 3.30(2)−4.04(2) Å; Na(1)B···C(22)B,C(27)B: 3.08(2)−3.90(2) Å.

(14) Zanotti-Gerosa, A.; Solari, E.; Giannini, L.; Floriani, C.; Chiesi-Villa, A.; Rizzoli, C. *Chem. Commun.* **1997**, 183.

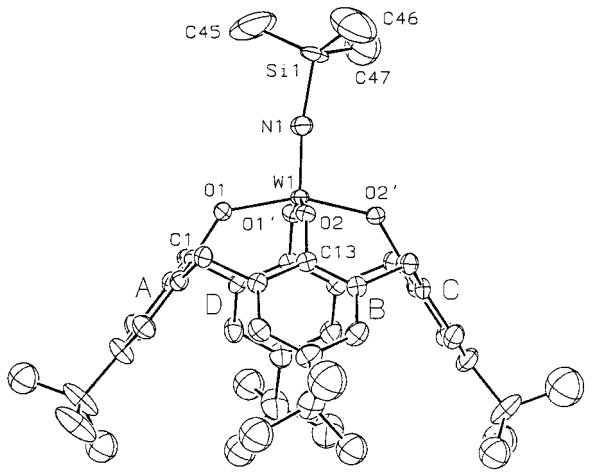

Figure 2. ORTEP drawing of complex **8** (50% probability ellipsoids). For the disordered atoms only the A position is given. A prime denotes a transformation of $-x, y, z$.

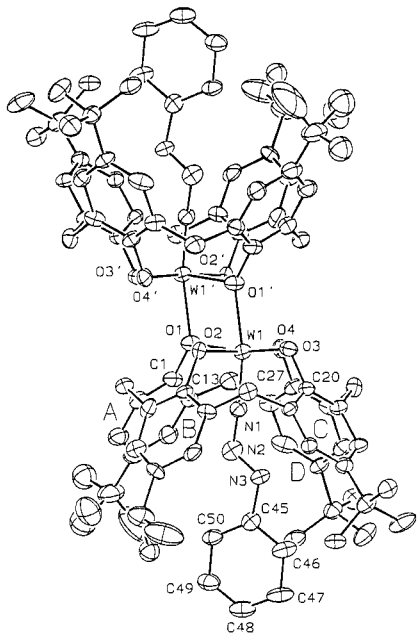

Figure 3. ORTEP drawing of molecule A in complex **12** (30% probability ellipsoids). For the disordered atoms only the A position is given. A prime denotes a transformation of $1-x, -y, -z$.

exo-bonding mode of the alkylimido derivative. In all four compounds **8**−**11**, the ^{1}H NMR spectrum shows a 4-fold symmetry of the calixarene fragment. The structural analysis of **8** (Figure 2) showed both the exo-position of the imido functionality and the strong W−N interaction.

Complex **8** possesses a crystallographically imposed C_m symmetry, the mirror plane running through the metal, N(1), and the C(14), C(28) bridging methylenic carbon atoms of the calixarene. The O_4 core is planar for symmetry requirements, so that the resulting coordination polyhedron around tungsten should be described as a regular square pyramid with the oxygen atoms of the core defining the base and the N(1) atom at the apex. The metal is displaced by 0.391(1) Å from the base toward N(1). The W−N vector [1.711(6) Å] is perpendicular to the O_4 plane, and the dihedral angle it forms with the normal to the base is 0.3(2)°. The $SiMe_3$ group was found to be statistically distributed about the mirror plane over two positions sharing the C(45) and C(46) methyl carbon atoms. As a consequence of the symmetry, the macrocycle assumes a spherical cone conformation (Table 3). The regularity of the conformation reflects the values of the two independent W−O bond distances that are not significantly different (Table 2). This conformation allows a toluene molecule to enter the cavity pointing the methyl group toward the metal [W···C(55), 4.530(17) Å].

The reaction of the phenyl azide with **2** led, however, to a completely different result, with the isolation of the metal-bonded azide inside the cavity of the calixarene ligand (see complex **12** in Scheme 2). The reaction proceeds with the two-electron reduction of the phenyl azide, as was also observed in the reaction with diphenyldiazomethane, forming a diazenylimido ligand. Two of them, $[V(N_3Mes)(I)(NRAr_F)_2]$[15] [R = CMe_3; Ar_F = 2,5-C_6H_3FMe; Mes = 2,4,6-$Me_3C_6H_2$] and $[Cp_2Ta(Me)(N_3$-Ar)],[16] are derived from the reaction of an aromatic azide with a d^2-metal. The solid-state structure of **12** (Figure 3) allows the structural parameters (Table 2) and the bonding mode of the azide functionality to be compared with those of the vanadium[15] and tantalum[16] derivatives. The structure of **12** will be described in detail jointly with that of **13** (see below).

Table 2. Comparison of Selected Bond Distances (Å) and Angles (deg) for Complexes 7, 8, 12, 13, and 15[a−d]

	7		8	12		13	15
W(1)−O(1)	2.028(11)	[2.060(12)]	1.919(3)	2.115(11)	[2.108(11)]	2.098(4)	2.253(5)
W(1)−O(2)	1.940(15)	[1.955(13)]	1.916(2)	1.945(12)	[1.914(13)]	1.936(5)	1.922(6)
W(1)−O(3)	2.023(12)	[2.027(12)]	1.916(2)	1.877(10)	[1.887(10)]	1.891(4)	1.931(5)
W(1)−O(4)	1.978(12)	[1.991(14)]	1.919(3)	1.923(12)	[1.913(12)]	1.929(5)	1.921(6)
W(1)−O(1)′				2.127(10)	[2.134(10)]	2.141(3)	2.061(5)
W(1)−N(1)	1.996(16)	[2.003(15)]	1.711(6)	1.749(11)	[1.735(11)]	1.717(4)	1.725(7)
	2.011(14)	[1.999(14)]					
N(1)−X	1.341(17)	[1.314(17)]	1.765(7)	1.314(17)	[1.342(16)]		1.404(12)
N(2)−C(45)	1.29(2)	[1.29(2)]					
N(2)−N(3)				1.27(2)	[1.26(2)]		
O(3)−W(1)−O(4)	82.0(5)	[81.4(5)]	87.5(1)	92.6(5)	[92.4(4)]	92.4(2)	83.5(2)
W(1)−O(1)−W(1)′				106.1(4)	[106.2(4)]	108.3(2)	113.9(2)
W(1)−N(1)−X	144.5(13)	[142.0(12)]	166.9(1)	171.2(11)	[169.8(12)]		172.8(7)
N(1)−N(2)−C(45)	126.0(15)	[125.7(16)]					
N(1)−N(2)−N(3)				116.0(12)	[114.4(11)]		
N(2)−N(3)−C(45)				112.8(12)	[111.7(12)]		

[a] For **8** O(3), O(4) should be read O(2)′, O(1)′ (′ = $-x, y, z$). [b] For **7** and **12** the values in the square brackets refer to molecule B. [c] A prime denotes a transformation of $1-x, -y, -z$ [$-x, 1-y, 1-z$]; $-x, -y, 1-z$; and $1-x, -y, -z$ for **12**, **13**, and **15**, respectively. [d] X should be read N(2), Si(1), N(2), and C(45) for **7**, **8**, **12**, and **15**, respectively.

Scheme 3

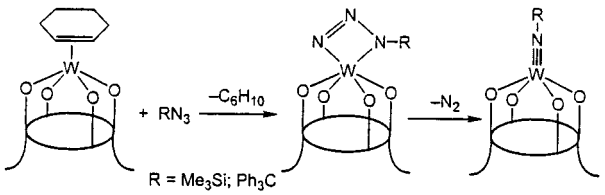

The apparent discrepancy due to the different kinds of compounds forming as a function of the R substituent at the azide gave significant support to the reported mechanism[16] of the metal-assisted formation of an aryl−alkyl-imido group from organic azides.

The major difference between the three azides we employed (see Scheme 2), namely, Me_3SiN_3, Ph_3CN_3, and PhN_3, depends on their tendency to react either on the metal-oxo surface (exo-mode) or inside the calixarene cavity (endo-mode). In the case of Ph_3C and Me_3Si substituents, the azide reacts via an exo-attack at the metal. The steric hindrance of the substituent can explain this kind of stereochemistry. In the exo-conformation, the metal-oxo surface provides the two *cis*-coordination sites, required by Bergman's mechanism,[16] and which foresees the 1,3-addition of the azide to the metal carbenoid. Then, the metallatriazacyclobutene undergoes N_2 extrusion (see Scheme 3), thus forming the corresponding alkylimido derivative. In the case of the endo-binding, as we found for PhN_3, the reaction led to the formation of the diazenylimido ligand in **12**, which, even upon heating, does not decompose to the corresponding phenylamido derivative. It should be emphasized at this point that the exo- vs endo-binding of a substrate in metallacalixarene corresponds to the possible selection of its reaction pathway.

The reaction of **2** with $Ph(Me)_2CN_3$ and HN_3 revealed another facet of the reactivity of metal azides. In both cases, the same compound, **13**, was formed (Scheme 2). The reaction of **2** with $Ph(Me)_2CN_3$ was, in fact, carried out at 60 °C, and the organic byproduct identified was α-methylstyrene. Under those conditions, we should admit that the organic azide is a source of HN_3, which is slowly released with the concomitant formation of α-methylstyrene. The generation of the imido (NH) inside the calixarene cavity seems intriguing, and in the present case we cannot invoke any 1,3-addition of the metal to the N_3 skeleton. We can suggest, in the case of HN_3, a preliminary bonding mode to the metal inside the calixarene cavity by the protonated nitrogen, which is the most basic one. Such a bonding mode, though proposed sometimes in organic azide−metal chemistry,[16] has never been proved. There is, however, a major difference between organic azides and HN_3. It is known that the protonation of HN_3 leads to $H_2N-N\equiv N$.[17] Therefore, the preliminary binding of HN_3 to the acidic metal would be followed by the extrusion of N_2 and the formation of the imido species, **13**. The formation of the imido functionality inside the calixarene cavity, as in the case of the analogous complex **12**, accompanies the dimerization of the W-calixarene unit via a bridging oxygen.

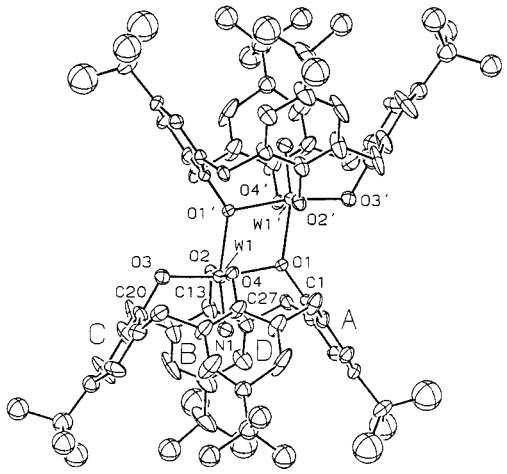

Figure 4. ORTEP drawing of complex **13** (50% probability ellipsoids). For the disordered atoms only the A position is given. A prime denotes a transformation of $-x, -y, 1-z$.

ORTEP drawings for **12** and **13** are given in Figures 3 and 4, respectively. The structures consist of neutral complex molecules originating from the bridging role of two O(1) oxygen atoms of the centrosymmetric calixarene ligands linking two [(*p*-Bu^t-calix[4]arene)W] units into a dimer. In complex **12**, two crystallographically independent "half-dimers" are present (called molecule

Table 3. Comparison of Relevant Conformational Parameters within the [W(calixarene)] Units for Complexes 7, 8, 12, 13, and 15

	7			**12**			
	mol A	mol B	**8**	mol A	mol B	**13**	**15**
(a) Distances (Å) of Atoms from the O_4 Mean Plane							
O(1)			0.0(−)	−0.062(10)	−0.055(11)	−0.028(3)	−0.358(4)
O(2)			0.0(−)	0.052(9)	0.050(10)	0.039(4)	0.395(4)
O(3)			0.0(−)	−0.053(9)	−0.051(10)	−0.039(4)	−0.417(4)
O(4)			0.0(−)	0.053(9)	0.045(10)	0.046(4)	0.399(4)
W			0.391(1)	0.113(1)	0.117(1)	0.146(1)	0.832(1)
(b) Dihedral Angles (deg) between Planar Moieties[a]							
E ^ **A**	168.4(4)	166.9(4)	125.6(1)	123.4(4)	123.5(5)	121.3(2)	113.3(2)
E ^ **B**	116.5(4)	118.1(5)	125.9(1)	117.1(4)	116.0(4)	123.4(2)	127.2(2)
E ^ **C**	159.4(4)	159.1(5)	125.9(1)	125.0(4)	125.6(4)	126.3(2)	161.3(2)
E ^ **D**	120.9(4)	123.0(4)	125.6(1)	118.0(5)	118.2(4)	118.9(2)	126.0(2)
A ^ **C**	147.9(6)	146.1(6)	108.5(2)	111.6(5)	110.9(6)	112.4(3)	94.6(3)
B ^ **D**	122.6(5)	118.9(6)	108.5(2)	124.1(5)	125.8(5)	117.6(3)	106.3(3)
(c) Contact Distances (Å) between *para*-Carbon Atoms of Opposite Aromatic Rings							
C(4)···C(17)	10.60(5)	7.71(3)	8.477(8)	8.63(2)	8.71(2)	8.630(13)	7.955(16)
C(10)···C(24)	10.57(5)	7.88(3)	8.477(8)	7.88(2)	7.86(3)	8.07(2)	8.793(14)

[a] **E** (reference plane) refers to the least-squares mean plane defined by the C(7), C(14), C(21), C(28) bridging methylenic carbons. [b] For **8** O(3), O(4), C(17), C(24) should be read O(2)′, O(1)′, C(10)′, C(4)′ (′ = $-x, y, z$).

Scheme 4

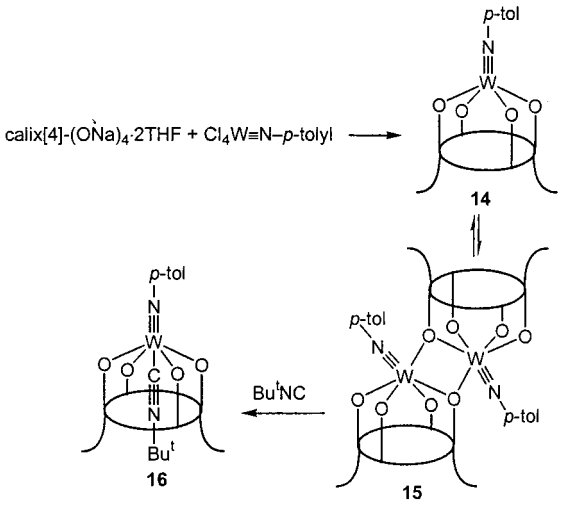

A and B); hereafter values in square brackets will refer to molecule B. The metal achieves the hexa-coordination through interaction with the tetrahedrally distorted O_4 core of calixarene, the O(1)′ oxygen atom of a symmetry-related macrocycle, and the nitrogen atom from an imido (**13**) or a diazenylimido (**12**) dianion hosted inside the cavity. The W−N bond distances (mean value 1.722(8) Å, Table 2) are consistent with the values expected for a W≡N triple bond. The resulting coordination polyhedra should be described as a distorted octahedron, for both complexes the best equatorial plane running through O(1), O(3), O(1)′, N(1) (a prime denotes a transformation of $1-x$, $-y$, $-z$ [$-x$, $1-y$, $1-z$] and $-x$, $-y$, $1-z$ for **12** and **13**, respectively). The W−O bond distances involving the O(2), O(3), O(4) atoms [mean value 1.912(8) Å] fall in a rather narrow range; those involving the bridging O(1) atoms [mean value 2.101(4) Å] are significantly longer. The macrocycles assume a regular cone conformation (Table 3).

The synthesis of phenylimido derivatives has so far been more easily achieved starting from the preformed functionality.[18] This can be made also in the case of tungsten, using $Cl_4W{\equiv}N-Ar$ as starting material to react with the calixarene sodium salt (see Scheme 4). The ^1H NMR spectrum shows, in solution, an equilibrium between a 4-fold, **14**, and a C_s, **15**, symmetry species in a molar ratio close to 1:1. When they are reacted with Bu^{t}NC, only the monomeric form of the isocyanide derivative **16** was found, both in solution and in the solid state. The monomeric imido−molybdenum and −tungsten complexes analogous to **14** or **16** have recently been reported to have been derived from synthetic methods close to that shown in Scheme 4. In such cases, with different substituents at the imido nitrogen, the dimerization has never been found.[18] From the solution containing both the monomeric **14** and the dimeric form **15**, the latter crystallized and its structure is shown in Figure 5. Unlike other phenylamido derivatives, the dimerization or the oligomerization does not involve the M≡N−R functionality.[19]

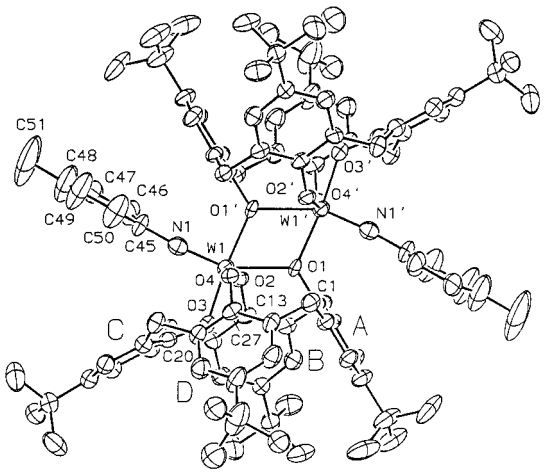

Figure 5. ORTEP drawing of the anion complex **15** (50% probability ellipsoids). For the disordered atoms only the A position is given. A prime denotes a transformation of $1-x$, $-y$, $-z$.

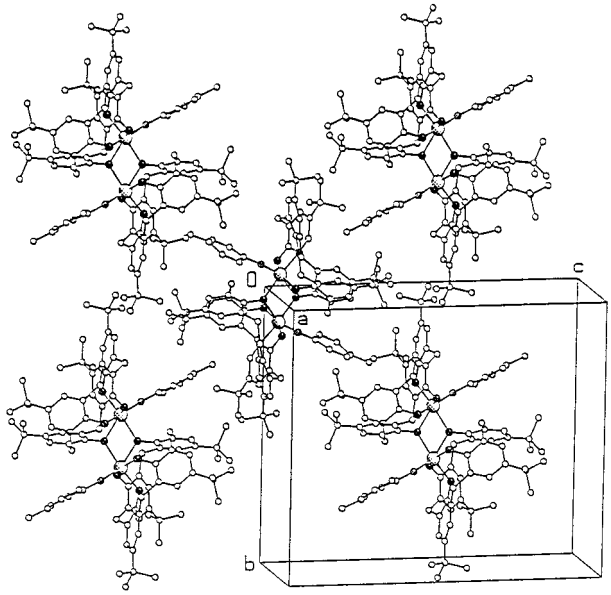

Figure 6. SCHAKAL view showing the packing of complex **15** along the (100) plane. For the disordered atoms only the A position is given.

Similarly for **12** and **13** the dimer takes its origin from the bridging role of the O(1) oxygen atoms from two centrosymmetric calixarene macrocycles (Figure 5). The *cis*-arrangement of the *p*-tolylimido group with O(1)′ (′ $=1-x$, $-y$, $-z$) gives rise to a remarkable deformation of the calixarene skeleton. This is indicated by the lack of planarity of the O_4 core and by the half-flattened conformation assumed by the macrocycle, in which the *C* ring is pushed outward with respect to the cavity coming out to be roughly parallel to the reference plane

(15) Fickes, M. G.; Davis W. M.; Cummins, C. C. *J. Am. Chem. Soc.* **1995**, *117*, 6384, and references therein.
(16) Proulx, G.; Bergman, R. G. *Organometallics* **1996**, *15*, 684, and references therein.
(17) Christe, K. O.; Wilson, W. W.; Dixon, D. A.; Khan, S. I.; Bau, R.; Metzenthin, T.; Lu, R. *J. Am. Chem. Soc.* **1993**, *115*, 1836.
(18) Radius U.; Attner, J. *Eur. J. Inorg. Chem.* **1999**, 2221, and references therein.
(19) (a) Solan, G. A.; Cozzi, P. G.; Floriani, C.; Chiesi-Villa, A.; Rizzoli, C. *Organometallics* **1994**, *13*, 2572. (b) Walsch, P. J.; Hollander, F. J.; Bergman, R. G. *J. Am. Chem. Soc.* **1988**, *110*, 8729. (c) Vroegop, C. T.; Teuben, J. H.; van Bolhuis, F.; van der Linden, J. G. M. *J. Chem. Soc., Chem. Commun.* **1983**, 550. (d) Green, M. L.; Hogarth, G.; Saunders: G. C. *J. Organomet. Chem.* **1991**, *421*, 233. (e) Green, M. L.; Leung, W.-H.; Ng, D. K. P. *J. Organomet. Chem.* **1993**, *460*, C4. (f) Walsch, P. J.; Hollander, F. J.; Bergman, R. G. *Organometallics* **1993**, *12*, 3705.

(Table 3). Tungsten exhibits a rather distorted octahedral coordination, the O(1), O(3), N(1), O(1)′ atoms defining the equatorial mean plane [maximum displacement 0.049(8) Å for N(1)]. The W−O bond distances fall in a narrow range [mean value 1.925(5) Å] except for the significant lengthening observed for the W−O(1) bond involving the bridging oxygen atom. Packing is mainly determined by the inclusion of PhMe fragments inside the cavities of two adjacent dimers. This gives rise to a chain running along the (100) plane (Figure 6).

Conclusions

The d^2-W-calixarene moiety weakly stabilized by a labile olefin ligand has been used for a two-electron reduction of nitrogen-rich substrates, namely, diphenyldiazomethane and organic azides. In the former case, the metallahydrazone derivative formed, while in the latter case two possible pathways have been observed depending on whether the reaction occurred at the metal either outside (exo) or inside (endo) the calixarene pocket. The exo reaction led to the alkylimido complexes, while in the endo case the diazenylimido ligand was generated inside the calixarene cavity. For the first time, we observed the calixarene cavity as being able to discriminate between two possible reaction pathways and to give substantial support to Bergman's mechanism on the metal-assisted decomposition of organic azides to alkyl- and arylimido functionalities.

Acknowledgment. We thank the "Fonds National Suisse de la Recherche Scientifique" (Bern, Switzerland, Grant No. 20-53336.98) and Action COST D9 (European Program for Scientific Research, OFES No. C98.008) for financial support.

Supporting Information Available: SCHAKAL drawings, tables giving crystal data and details of the X-ray data collection, structure solution, and refinement, atomic coordinates, isotropic and anisotropic displacement parameters, and bond length and angles for **7**, **8**, **12**, **13**, and **15**. This material is available free of charge via the Internet at http://pubs.acs.org.

OM000612S